Durham University

Durham Research Online

Deposited in DRO:

08 January 2020

Version of attached file:

Accepted Version

Peer-review status of attached file:

Peer-reviewed

Citation for published item:

Haase, Nils and Danos, Andrew and Pflumm, Christof and Morherr, Antonia and Stachelek, Patrycja and Mekic, Amel and Brütting, Wolfgang and Monkman, Andrew P. (2018) 'Kinetic modeling of transient photoluminescence from thermally activated delayed fluorescence.', Journal of physical chemistry C., 122 (51). pp. 29173-29179.

Further information on publisher's website:

https://doi.org/10.1021/acs.jpcc.8b11020

Publisher's copyright statement:

This document is the Accepted Manuscript version of a Published Work that appeared in final form in Journal of physical chemistry C copyright © American Chemical Society after peer review and technical editing by the publisher. To access the final edited and published work see https://doi.org/10.1021/acs.jpcc.8b11020

Additional information:

Use policy

The full-text may be used and/or reproduced, and given to third parties in any format or medium, without prior permission or charge, for personal research or study, educational, or not-for-profit purposes provided that:

- a full bibliographic reference is made to the original source
- a link is made to the metadata record in DRO
- the full-text is not changed in any way

The full-text must not be sold in any format or medium without the formal permission of the copyright holders.

Please consult the full DRO policy for further details.

Durham University Library, Stockton Road, Durham DH1 3LY, United Kingdom
Tel : +44 (0)191 334 3042 | Fax : +44 (0)191 334 2971
https://dro.dur.ac.uk

THE JOURNAL OF PHYSICAL CHEMISTRY C

Subscriber access provided by UNIV OF DURHAM

C: Energy Conversion and Storage; Energy and Charge Transport

Kinetic Modelling of Transient Photoluminescence from Thermally Activated Delayed Fluorescence

Nils Haase, Andrew Danos, Christof Pflumm, Antonia Morherr, Patrycja Stachelek, Amel Mekic, Wolfgang Brutting, and Andrew P. Monkman

J. Phys. Chem. C, **Just Accepted Manuscript** • DOI: 10.1021/acs.jpcc.8b11020 • Publication Date (Web): 03 Dec 2018

Downloaded from http://pubs.acs.org on December 4, 2018

Just Accepted

"Just Accepted" manuscripts have been peer-reviewed and accepted for publication. They are posted online prior to technical editing, formatting for publication and author proofing. The American Chemical Society provides "Just Accepted" as a service to the research community to expedite the dissemination of scientific material as soon as possible after acceptance. "Just Accepted" manuscripts appear in full in PDF format accompanied by an HTML abstract. "Just Accepted" manuscripts have been fully peer reviewed, but should not be considered the official version of record. They are citable by the Digital Object Identifier (DOI®). "Just Accepted" is an optional service offered to authors. Therefore, the "Just Accepted" Web site may not include all articles that will be published in the journal. After a manuscript is technically edited and formatted, it will be removed from the "Just Accepted" Web site and published as an ASAP article. Note that technical editing may introduce minor changes to the manuscript text and/or graphics which could affect content, and all legal disclaimers and ethical guidelines that apply to the journal pertain. ACS cannot be held responsible for errors or consequences arising from the use of information contained in these "Just Accepted" manuscripts.

ACS Publications

is published by the American Chemical Society. 1155 Sixteenth Street N.W., Washington, DC 20036

Published by American Chemical Society. Copyright © American Chemical Society. However, no copyright claim is made to original U.S. Government works, or works produced by employees of any Commonwealth realm Crown government in the course of their duties.

Kinetic Modelling of Transient Photoluminescence from Thermally Activated Delayed Fluorescence

*Nils Haase** [a,b], *Andrew Danos** [c], *Christof Pflumm* [b], *Antonia Morherr* [b], *Patrycja Stachelek* [c], *Amel Mekic* [b,d], *Wolfgang Brütting* [a], *and Andrew P. Monkman* [c]

[a] Institute of Physics, Experimental Physics IV, University of Augsburg, Universitätsstr. 1, 86135 Augsburg, Germany

[b] Merck KGaA, Performance materials - Display Solutions, Frankfurter Straße 250, 64293 Darmstadt, Germany

[c] Department of Physics, Durham University, South Road, DH1 3LE, UK

[d] Institute of Organic Chemistry, University of Regensburg, Universitätsstr. 31, 93053 Regensburg, Germany

*Email: nils.haase@external.merckgroup.com
*Email: andrew.danos@durham.ac.uk

Abstract

A simplified state model and associated rate equations are used to extract the reverse intersystem crossing and other key rate constants from transient photoluminescence measurements of two high performance thermally activated delayed fluorescence materials. The values of the reverse intersystem crossing rate constant are in close agreement with established methods, but do not require *a priori* assumption of exponential decay kinetics, nor any additional steady state measurements. The model is also applied to measurements at different temperatures and found to reproduce previously reported thermal activation energies for the thermally activated delayed fluorescence process. Transient absorption measurements provide independent confirmation that triplet decay channels (neglected here) have no adverse effect on the fitting.

Introduction

In contrast to phosphorescent iridium or triplet-triplet annihilation (TTA) based organic light emitting diodes (OLEDs), devices that harvest triplet excitons using thermally activated delayed fluorescence (TADF) promise to deliver deep blue emission and internal quantum efficiencies (IQE) up to 100% while also avoiding the use of precious metals[1-9]. TADF materials rely on a small energy splitting between the lowest excited singlet and triplet states (ΔE_{ST}), such that thermally activated reverse intersystem crossing (rISC) can promote the upconversion of non-emissive triplet states.

While considerable work has been done to design highly efficient TADF molecules with a small ΔE_{ST}, examples of poor TADF compounds with very low ΔE_{ST} demonstrate that it is not the only relevant design factor[10]. Instead, the true criterion for efficient TADF is simply a large rISC rate constant (k_{rISC}). Despite this central importance, no practical yet theoretically sound method for the determination of k_{rISC} as part of the routine characterization of TADF materials has been provided - until now.

Unfortunately, a direct measurement of k_{rISC} is difficult and requires complex modelling of ultrafast transient absorption[11]. Nonetheless, various indirect approaches exist to describe the kinetic behavior of TADF molecules and obtain approximate values of k_{rISC}. Early on, TADF materials were described in terms of the equilibrium model[12-13]. More recently, Dias et al.[14] estimated k_{rISC} from the photoluminescence quantum yields (PLQY) and exponential lifetimes of the prompt fluorescence and the delayed fluorescence via

$$k_{rISC} = \frac{1}{\tau_{DF}} \frac{\Phi_{PF} + \Phi_{DF}}{\Phi_{PF}} = \frac{1}{\tau_{DF}}\left(1 + \frac{I_{DF}}{I_{PF}}\right) \quad (1)$$

where τ_{DF} is the lifetime of the delayed fluorescence, Φ_{PF} is the photoluminescence quantum yield of the prompt fluorescence and Φ_{DF} the photoluminescence quantum yield of the delayed fluorescence. This can also be expressed in terms of I_{DF}/I_{PF}, the ratio of total emission signal from delayed and prompt emission. In deriving equation (1) the assumption is made that non-radiative processes from the triplet state are suppressed such that $\Phi_{rISC} \approx 1$, which is ensured when $\Phi_{DF}/\Phi_{PF} \gtrsim 4$[14].

Two experimental approaches exist to evaluate equation (1), although neither can be universally applied. Common to both methods, time resolved emission measurements must be made and exponential fitting performed to determine τ_{DF}. While this process is often straightforward, identifying the appropriate time region for fitting can be challenging in solid hosts, where an ensemble of TADF molecular geometries and microenvironments can result in complex multi-exponential decay in the delayed regime[15]. This is especially the case at low temperatures, where phosphorescence emission can compete with inhibited TADF. Exponential fitting is then also applied in the prompt region, allowing I_{DF}/I_{PF} to be evaluated as the ratio of areas bound by the fitted exponential curves in the delayed and prompt regions.

Alternatively, steady state measurements can be compared in air and inert atmosphere. By assuming that oxygen fully quenches all triplet states and thus any delayed emission, the ratio $(\Phi_{PF} + \Phi_{DF})/\Phi_{PF}$ can be replaced by the ratio of PLQYs or total emission intensities in vacuum (PF and DF), and in air (PF only). This assumption does not hold in all circumstances though, as high performance TADF materials may have rISC rates large enough to compete with oxygen quenching, while some hosts can restrict oxygen diffusion and its ability to quench triplets in a

solid film. Any additional Φ_{DF} contribution to the oxygenated measurement results in an underestimate of k_{rISC}, and is exacerbated when k_{rISC} is already large.

Although applied successfully elsewhere[14, 16], both methods of evaluating equation (1) ultimately rely on partitioning the emission decay kinetics into prompt and delayed regions for fitting.* While Adachi and coworkers have recently reported three and four level TADF models that indeed have exponential analytic solutions, the interaction of population dependent emission, ISC, and rISC rates means that the fitted exponential prefactors and decay rates are highly interlinked. In this framework equation (1) is revealed to lack a sound theoretical basis and is at best an approximation (albeit a very useful and successful one). Instead, challenging algebra is required to relate the fitting parameters of these analytic solutions to the rate constants of interest, which limits the practicality of this approach. Focusing only on the most delayed rate constant can simplify analysis, but at the cost of discarding any fitting power available through the prompt decay data. We also reiterate that in practice it is rarely possible to unambiguously identify separate regions for exponential fitting in the first place - a prerequisite for any analytic approach[17-18].

In contrast to the approaches above, Penfold et al. recently considered the TADF mechanism as a kinetic process, which allows rapid extraction not only of rate constants but also time dependent state populations from transient photoluminescence experiments[19]. Here, we apply

*It is instructive to note the parallel development of TADF and TTA research, both of which involve prompt and delayed emission components that can be modelled with biexponential decays. For TTA the fast and slow processes correspond to second and first order decay mechanisms operating on the same triplet population. Differential equations (some with convenient analytic solutions) have widely replaced the use of exponential fitting for TTA, enabling the annihilation rate constant to be reliably determined [17,18]. Here we apply similar methods to TADF.

this model to obtain values of k_{rISC} and other key rate constants from time-resolved photoluminescence measurements of two high performance D-A-D TADF materials. Additionally, applying the kinetic model to data taken at different temperatures allows us to determine the activation energies of TADF in these materials, which are in close agreement with previously determined values.

Methods and Kinetic Model

In photoluminescence experiments, there are usually two channels to optically excite a D-A or D-A-D TADF molecule. Excitons can be generated on a local excited singlet state (^{1}LE) via a strong local donor (or acceptor) π-π^* transition [20], which can then either decay radiatively or undergo electron transfer to form a singlet charge transfer state (^{1}CT). Alternatively, the ^{1}CT state can be excited directly through a weak (n-π^*/ π-π^*) mixed transition [14]. Since both ^{1}LE and ^{1}CT have fast radiative decay rates, simultaneous emission typically occurs for the first ~5 ns [14]. For later times the ^{1}LE contribution to the emission spectra vanishes while ^{1}CT emission persists as the ^{1}CT state is continually repopulated by TADF. Therefore, only one singlet state (S_1) is directly considered in the simplified rate model presented here (shown in the right of Figure 1). To evaluate the contribution of the ^{1}LE emission at early times the initial population of the singlet state $[S_1](t=0)$ is taken as an additional fit parameter.

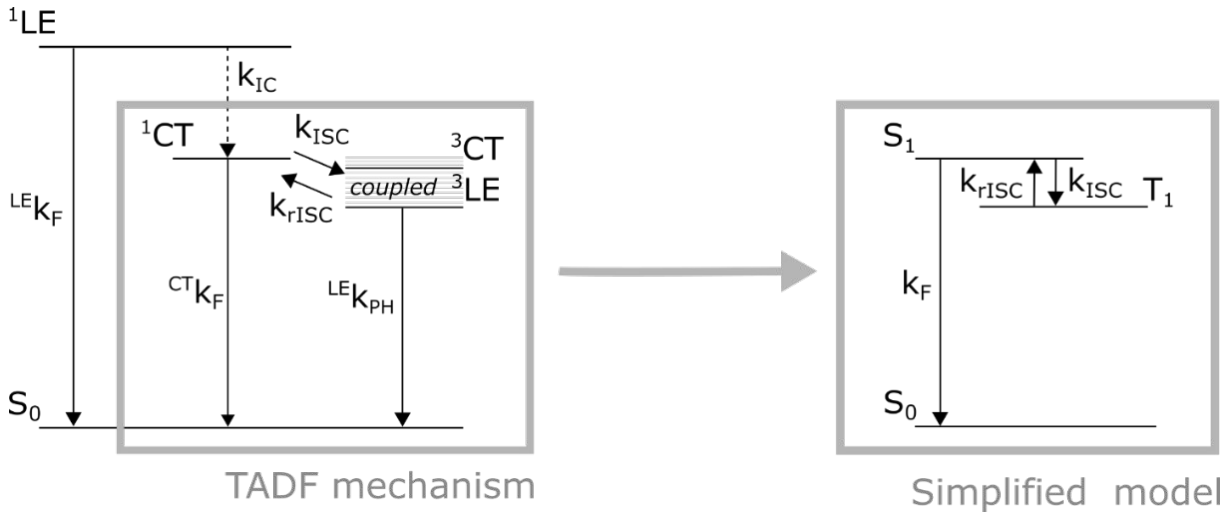

Figure 1: Left: Schematic representation of the energy levels and rate constants that govern TADF kinetics. Right: Simplified model used to extract rate constants and state populations.

The TADF mechanism itself is based on a complex four-state model, shown in the left grey box of Figure 1, where the ^{1}CT, ^{3}CT and ^{3}LE states are mixed through a second order coupling [21-24]. Once the excited ^{1}CT state is formed it can either decay radiatively yielding prompt ^{1}CT fluorescence emission, or it can populate the ^{3}LE state via intersystem crossing (ISC). Both non-adiabatic coupling and thermal energy then lead to mixing and formation of equilibrium populations in ^{3}CT and ^{3}LE, at rates far exceeding that of spin-orbit coupling (SOC) between the ^{1}CT and ^{3}LE state [22, 25]. Indeed, calculations by Gibson and Penfold show that the equilibrium between ^{3}CT and ^{3}LE is only very weakly temperature dependent [25] and that for small energy gaps between those two states the non-adiabatic vibronic coupling is strong enough to populate the ^{3}CT state even at 0 K. Consequently, we consider only one mixed triplet state (T_1) as the lowest lying triplet state in the simplified TADF model. Slow phosphorescence and non-radiative pathways are not considered in this model, justified by transient absorption measurements presented further below. As is necessary in deriving equation (1), this is equivalent to assuming $\Phi_{rISC} \approx 1$.

The simplified model of the TADF process forms a system of linear differential equations:

$$\frac{d[S_1]}{dt} = -(k_F + k_{ISC})[S_1] + k_{rISC}[T_1] \quad (2)$$

$$\frac{d[T_1]}{dt} = k_{ISC}[S_1] - k_{rISC}[T_1] \quad (3)$$

The time-dependent rate model is solved numerically using the `odeint` function from the SciPy library in Python 3.6 for specific values of k_F, k_{ISC}, k_{rISC} and $[S_1](t=0)$, with $[T_1](t=0)$ set to zero. To extract the rate constants and state population kinetics, we fit $[S_1]$ to normalized data of transient photoluminescence experiments using the `curve_fit` tool from SciPy. Since S_1 is the only emissive state in the considered model, its population is directly proportional to the photoluminescence emission intensity. The implementation of this fitting model is presented in detail in the supporting information, with particular attention given to methods of parameter optimization and sensitivity to starting values.

Results and Discussion

Using the kinetic model discussed above, we analyzed the kinetics of the D-A-D TADF molecules DDMA-TXO2 [26-27] and DPTZ-DBTO2 [14] in solid state. Both emitters show clear delayed emission and give excellent device performances with maximum external quantum efficiencies (EQE) above 18%. Figure 2 shows the emission decay from the early prompt emission to the end of the delayed fluorescence of DPEPO:DDMA-TXO2(13 vol% emitter in host) at 290 K taken from ref. [26] and CBP:DPTZ-DBTO2(10%) at 298 K taken from ref. [14]. In addition, the fitted time dependent singlet and calculated triplet populations are shown, and are

found to accurately reproduce independent transient absorption measurements presented in Figure 5. The best fit results obtained are shown in Table 1.

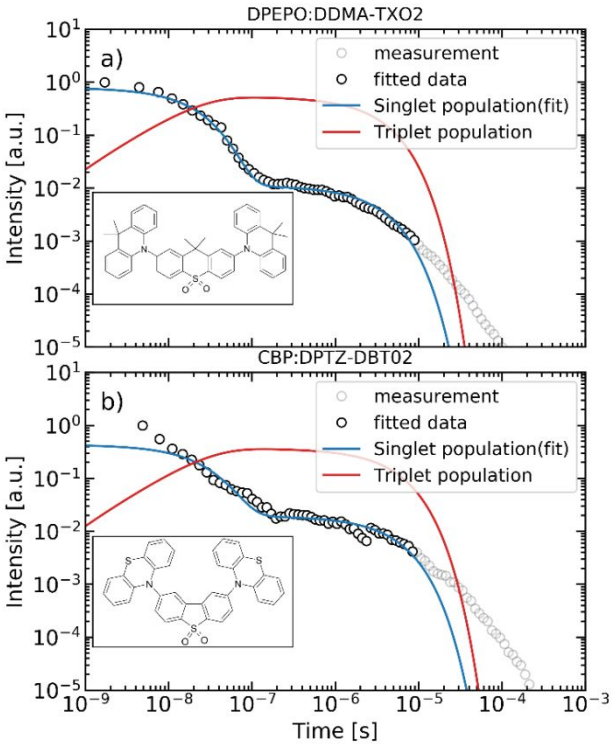

Figure 2: Structures (inset) and emission decay (black circles) of a) DPEPO:DDMA-TXO2(13%)[26] and b) CBP:DPTZ-DBTO2(10%) [14] at room temperature. Also shown are the fitted time dependent singlet (blue) and calculated triplet populations (red) for each emitter. Grey data points are not included in the fits shown, but are found to have negligible influence on the final fit parameters as discussed in the SI.

For both materials the singlet population accurately describes the emission decay for several orders of magnitude and shows clear prompt and delayed contributions. The singlet population is not in good agreement with the recorded emission only at very early and very late times. At very early times the emission is a combination of fluorescence from ^{1}CT and ^{1}LE [14]. Supporting this, Figure 3 shows an additional contribution to the total emission in the spectra for both samples at

early times, presumably from the ^{1}LE emission of the donor unit. For DPEPO:DDMA-TXO2(13%) the ^{1}CT emission is already dominant at 3.5 ns, while the major contributor to emission for CBP:DPTZ-DBTO2(10%) is the ^{1}LE state until at least 7.8 ns. This observation is consistent with the fit values of $[S_1](t=0)$, 78.4% for DPEPO:DDMA-TXO2(13%) and 43.1% for CBP:DPTZ-DBTO2(10%), which represent the proportion of the initial total emission intensity that originates from the ^{1}CT state. After about 18 ns the ^{1}LE contribution to the emission spectra vanishes for both materials, and the kinetic model begins to accurately describe the experiment.

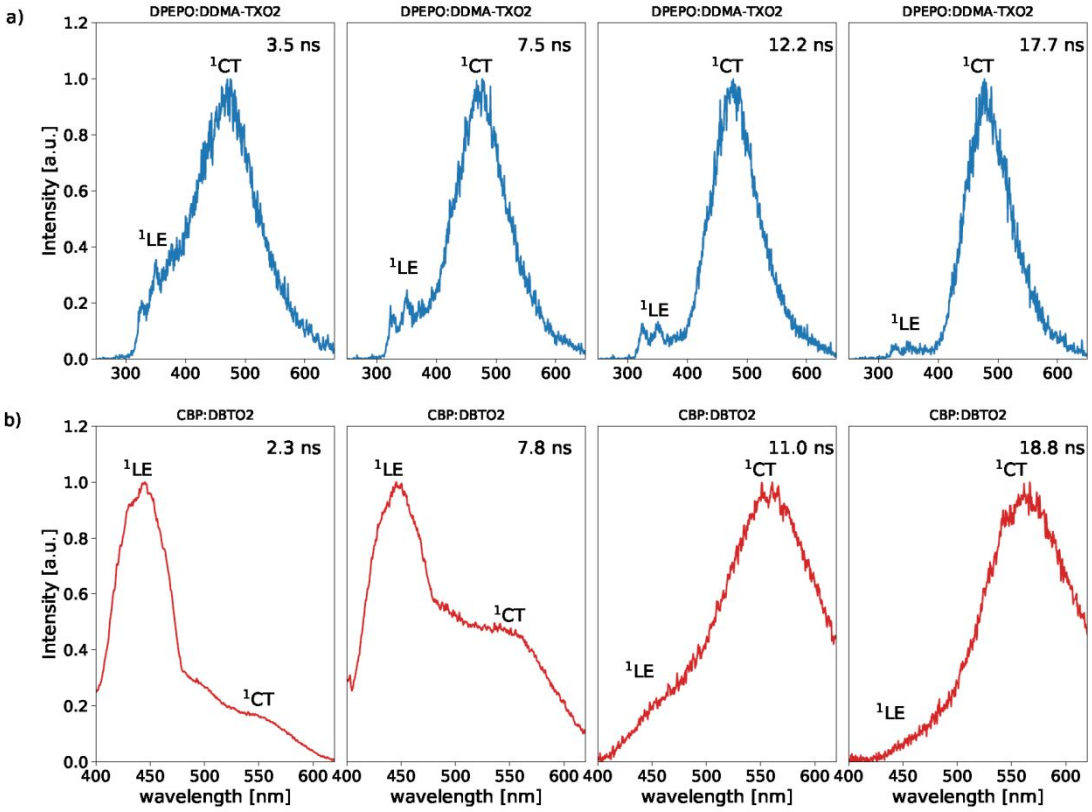

Figure 3: Time resolved emission spectra of a) DPEPO:DDMA-TXO2(13%) and b) CBP:DPTZ-DBTO2(10%), obtained at very early times following the excitation.

The additional emission at very late times can be attributed to long living but weak emission from a small subset of molecules which cannot undergo rapid rISC due to unfavorable D-A angles [14]. An ensemble of different D-A angles is expected to give rise to an ensemble of k_{rISC} values and the resulting power law behavior (appearing linear on a log-log scale). As the validity of the kinetic modelling is concerned, we note that the overall intensity in this regime is exaggerated by the log-log figure axes, and is both relatively and absolutely small. Furthermore, we also find that the fitted rate constants are insensitive to the inclusion or exclusion of this tail region, as detailed in the supporting information. Nonetheless, a decisive advantage of our kinetic approach compared to existing ones is that equation (3) can be readily modified or expanded to treat an ensemble of rISC rates as needed in future.

Figure 4 shows the temperature dependence of emission decays from the films of DPEPO:DDMA-TXO2(13%) and CBP:DPTZ-DBTO2(10%) (taken from [26] and [14]) together with the fitted singlet population. The changes with temperatures for DPEPO:DDMA-TXO2(13%) are relatively small compared to the CBP:DPTZ-DBTO2(10%) sample, qualitatively indicative of a smaller energy gap for DPEPO:DDMA-TXO2(13%). The best fit results obtained for the different temperatures and TADF emitters are shown in Table 1. For all photoluminescence decays, the singlet population follows the experimental data over several orders of magnitude. Only at very early (<20 ns) and very late times (>10 μs), does the fit not describe the emission accurately, as discussed above. The values of k_{rISC} also compare well to those determined using equation (1) (I_{DF}/I_{PF} via areas method) for all evaluated temperatures, without requiring selection of segregated prompt and delayed regions. As the values for k_{rISC} are faithfully reproduced by our method, estimates of ΔE_{ST} derived from the changes in k_{rISC} with temperature will also agree with existing methods based on equation (1).

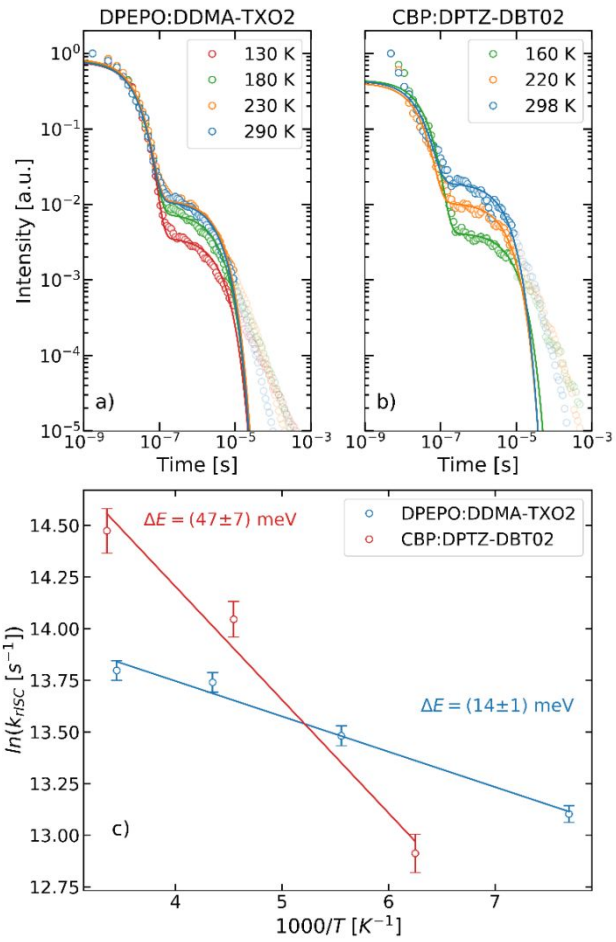

Figure 4: a,b: Emission decay of DPEPO:DDMA-TXO2(13%) and CBP:DPTZ-DBTO2(10%), as a function of temperature (circles), together with the fitted singlet population (lines). c: Arrhenius plot of k_{rISC} values fitted from the decays. Greyed data points are not included in the fits shown.

We also find that k_{ISC} increases with increasing temperature in a similar fashion to k_{rISC}. In contrast, k_F is found to decrease with increasing temperature for both materials. This decrease cannot be the result of an unmodeled temperature dependent increase of non-radiative rate constants, as the PLQY of DPEPO:DDMA-TXO2(13%) at room temperature is as high as 95±5% [26]. To explain this trend we suggest that the average D-A dihedral angle is temperature dependent, and shifts closer to orthogonality at higher temperatures. This change in geometry

reduces the overlap between donor and acceptor groups, leading to the observed increase in k_{ISC} and reduction in k_F [15].

The initial state population $[S_1](t=0)$ shows no temperature dependence for either sample, with values consistently higher for DPEPO:DDMA-TXO2(13%) compared to CBP:DPTZ-DBTO2(10%). This difference reflects the larger initial contribution of ^{1}LE to the emission of the CBP:DPTZ-DBTO2(10%) film (Figure 3), determined by both the competition of rates for ^{1}LE emission and electron transfer (to form CT states), as well as the ratio of ^{1}LE and direct ^{1}CT absorption using 355 nm excitation. Neither of these factors are expected to be temperature sensitive. Instead we find that the fitted value of $[S_1](t=0)$ is highly sensitive to the selection of the initial data point for normalization - in both materials rising to 100% when chosen at times after ^{1}LE emission increases. Indeed, while we employ $[S_1](t=0)$ as a fitting parameter here, alternate future implementations may instead set its value by careful comparison of ^{1}CT and ^{1}LE intensities in the earliest spectrum of a decay series (for molecules where these emissions are easily resolvable). We also find improved fitting at early times if only the wavelengths corresponding to ^{1}CT emission are integrated to generate decay curves.

The values of k_{rISC} are found to display Arrhenius-like behavior as shown in Figure 3c, the gradient of which is used to determine the activation energy of rISC. We obtain an activation energy of (14±1) meV for the DPEPO:DDMA-TXO2(13%) and (47±3) meV for the CBP:DPTZ-DBTO2(10%) sample, respectively, analogous to Arrhenius analysis of delayed emission intensity employed by others [8, 14, 25]. These values are close to those determined from the optical energy gap ΔE_{ST} calculated from the energy difference between the onset of the ^{1}CT and ^{3}LE emission as described elsewhere[26], which are reported as (10±3) meV for DPEPO:DDMA-TXO2(13%) and (20±4) meV for CBP:DPTZ-DBTO2(10%) [14, 26], respectively.

Since the activation energy and the energy gap extracted from the emission onset describe the energy difference between different states of the TADF process, it has been repeatedly found that the calculated energy gap differs between these approaches, especially for better performing molecules [3].

Table 1: Fitted rate constants, and k_{rISC} values determined using Dias method.

DPEPO:DDMA-TXO2(13%)

temp. [K]	$[S_1](t=0)$[%]	k_F [10^6 s^{-1}]	k_{ISC} [10^6 s^{-1}]	k_{rISC} [10^5 s^{-1}]	k_{rISC} [10^5 s^{-1}] by Dias et al. [14]
290	78.4 ± 0.1	15.0 ± 0.3	32.4 ± 1.2	9.8 ± 0.3	10.8
230	83.6 ± 5.5	14.4 ± 0.8	31.5 ± 1.2	9.3 ± 0.4	10.0
180	80.6 ± 5.6	18.4 ± 1.0	26.7 ± 1.0	7.1 ± 0.3	8.0
130	78.3 ± 4.6	26.0 ± 1.1	20.6 ± 0.7	4.9 ± 0.2	5.4

CBP:DPTZ-DBTO2(10%)

temp. [K]	$[S_1](t=0)$[%]	k_F [10^6 s^{-1}]	k_{ISC} [10^6 s^{-1}]	k_{rISC} [10^5 s^{-1}]	k_{rISC} [10^5 s^{-1}] by Dias et al. [14]
298	43.1 ± 5.1	4.0 ± 0.5	33.4 ± 3.2	19.3 ± 2.0	18.1
220	40.7 ± 4.1	6.1 ± 0.7	34.3 ± 2.4	12.6 ± 1.0	12.9
160	44.1 ± 3.6	8.8 ± 0.9	20.7 ± 1.1	4.1 ± 0.3	4.6

Finally, we reiterate that the approach above does not consider any triplet decay (radiative or non-radiative), as justified at first by absence of phosphorescence spectra in the decays and the quality of subsequent fits. Independent justification for this approach is given by transient absorption (TA) measurements of both materials at room temperature shown in Figure 5 (blue circles). Also included are the emission decay data and with fitted triplet and singlet populations from fitting (identical to Figure 2). Descriptions of the sample preparation, TA apparatus, and data processing are included in the supporting information. Strong and long lived TA signal

consistent with photogenerated triplet states were observed at 600 nm for DPEPO:DDMA-TXO2(20%) and 650nm for CBP:DPTZ-DBTO2(20%).

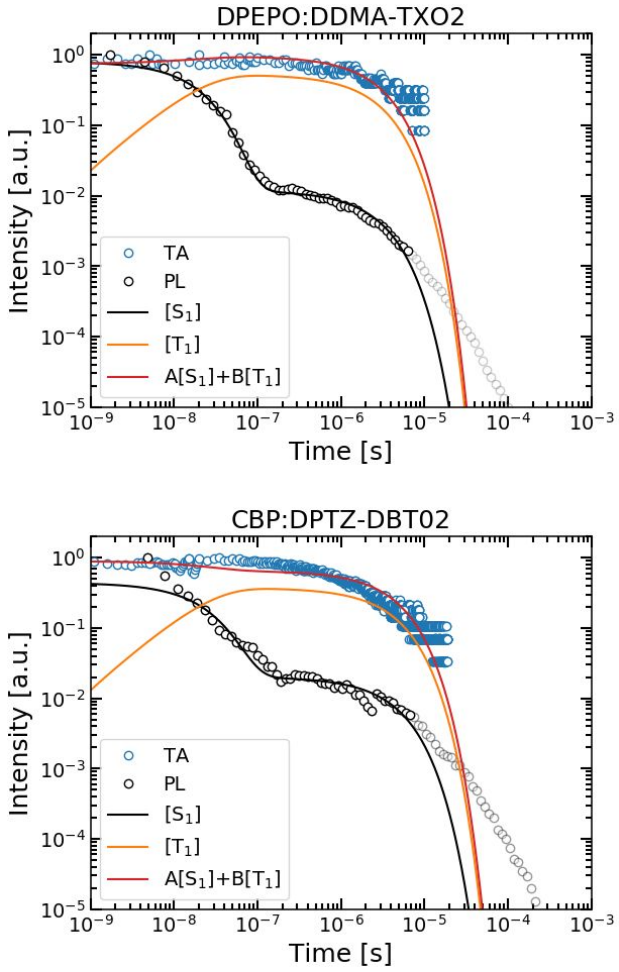

Figure 5: Transient absorption data (TA), along with independently measured and fitted emission (PL) decay. Linear combinations of the singlet and triplet populations from fitted photoluminescence decays ($A[S_1] + B[T_1]$) are able to accurately reproduce the experimental absorption data.

We find that the TA data can be reproduced from a linear combination of the triplet and singlet populations generated only from the PL decay. The best fits are shown as red lines in Figure S4, and come from $0.89[S_1] + 0.59[T_1]$ for DPEPO:DDMA-TXO2(20%) and $0.75[S_1] + 0.9[T_1]$ for

CBP:DPTZ-DBTO2(20%), although these values are somewhat meaningless as all populations and the TA data itself are individually normalized.

We interpret the fact that the TA signal can be fit using linear combinations of $[S_1]$ and $[T_1]$ as evidence that it consists of contributions from short lived $S_1 \rightarrow S_n$ and long lived $T_1 \rightarrow T_n$ transitions. Critically, the good agreement of the TA data at long times (coming from triplet absorptions) with the $[T_1]$ population from emission decay fitting demonstrates that the fitted $[T_1]$ accurately describe the actual triplet population kinetics in the material. Since the fitted $[T_1]$ curves are generated without inclusion of kinetic terms for triplet radiative or non-radiative decay, the agreement with TA measurements confirms that these processes are indeed negligible for these materials.

Nonetheless, future work on other materials or at low temperatures may require triplet decay to be explicitly addressed. In these circumstances we identify that equation (3) is readily expandable to include these processes with additional terms, for example:

$$\frac{d[T_1]}{dt} = k_{ISC}[S_1] - (k_{rISC} + k_{PH} + k_{nr})[T_1] \quad (4)$$

and that emissive decay from ^{1}CT and ^{3}LE can usually be resolved spectrally. Identifying when modifications like equation (4) are necessary may require access to transient absorption, although comparing fitted values of k_{rISC} fit using equation (3) with $k_{PH} + k_{nr}$ (from the inverse of a measured phosphorescence lifetime) may also suffice when absorption measurements are impractical.

Conclusion

We have shown that fitting of transient photoluminescence experiments with a simplified kinetic model yields reliable values for the relevant rate constants of the TADF process. A key parameter for the photophysical characterization, the reverse intersystem crossing rate constants are determined with values of k_{rISC} = 9.8x10^5 s^{-1} for **DPEPO:DDMA-TXO2(13%)** and k_{rISC} = 1.93x10^6 s^{-1} for **CBP:DPTZ-DBTO2(10%)** at room temperature, without the need for additional steady state measurements nor choice of a delayed region for exponential fitting. In addition, the model gives the time dependent populations of the singlet and triplet states, reproduces the activation energy of the rISC process from an Arrhenius plot, and due to its kinetic nature can be readily expanded to include rISC rate distributions and triplet decay. Since k_{rISC} is ultimately more important than ΔE_{ST} for high performance TADF materials we propose that the presented analysis should become standard for characterizing new TADF materials.

Supporting Information

Discussion of fitting method implementation, transient absorption data acquisition and processing

Acknowledgement

This research was supported by the HyperOLED project from the European Unions's Horizon 2020 research and innovation program under grant agreement number 732013.

References

1. Adachi, C.; Baldo, M. A.; Thompson, M. E.; Forrest, S. R., Nearly 100% Internal Phosphorescence Efficiency in an Organic Light-Emitting Device. *J. Appl. Phys.* **2001**, *90*, 5048-5051.

2. Baldo, M. A.; O'brien, D.; You, Y.; Shoustikov, A.; Sibley, S.; Thompson, M.; Forrest, S. R., Highly Efficient Phosphorescent Emission from Organic Electroluminescent Devices. *Nature* **1998**, *395*, 151.
3. Dias, F. B.; Bourdakos, K. N.; Jankus, V.; Moss, K. C.; Kamtekar, K. T.; Bhalla, V.; Santos, J.; Bryce, M. R.; Monkman, A. P., Triplet Harvesting with 100% Efficiency by Way of Thermally Activated Delayed Fluorescence in Charge Transfer Oled Emitters. *Adv. Mater.* **2013**, *25*, 3707-3714.
4. Jankus, V.; Data, P.; Graves, D.; McGuinness, C.; Santos, J.; Bryce, M. R.; Dias, F. B.; Monkman, A. P., Highly Efficient Tadf Oleds: How the Emitter–Host Interaction Controls Both the Excited State Species and Electrical Properties of the Devices to Achieve near 100% Triplet Harvesting and High Efficiency. *Adv. Funct. Mater.* **2014**, *24*, 6178-6186.
5. Kondakov, D.; Pawlik, T.; Hatwar, T.; Spindler, J., Triplet Annihilation Exceeding Spin Statistical Limit in Highly Efficient Fluorescent Organic Light-Emitting Diodes. *J. Appl. Phys.* **2009**, *106*, 124510.
6. Méhes, G.; Nomura, H.; Zhang, Q.; Nakagawa, T.; Adachi, C., Enhanced Electroluminescence Efficiency in a Spiro-Acridine Derivative through Thermally Activated Delayed Fluorescence. *Angew. Chem. Int. Edit.* **2012**, *51*, 11311-11315.
7. Sivasubramaniam, V.; Brodkorb, F.; Hanning, S.; Loebl, H. P.; van Elsbergen, V.; Boerner, H.; Scherf, U.; Kreyenschmidt, M., Fluorine Cleavage of the Light Blue Heteroleptic Triplet Emitter Firpic. *J. Flourine Chem.* **2009**, *130*, 640-649.
8. Uoyama, H.; Goushi, K.; Shizu, K.; Nomura, H.; Adachi, C., Highly Efficient Organic Light-Emitting Diodes from Delayed Fluorescence. *Nature* **2012**, *492*, 234.
9. Wang, H.; Xie, L.; Peng, Q.; Meng, L.; Wang, Y.; Yi, Y.; Wang, P., Novel Thermally Activated Delayed Fluorescence Materials–Thioxanthone Derivatives and Their Applications for Highly Efficient Oleds. *Adv. Mater.* **2014**, *26*, 5198-5204.
10. Etherington, M. K.; Gibson, J.; Higginbotham, H. F.; Penfold, T. J.; Monkman, A. P., Revealing the Spin–Vibronic Coupling Mechanism of Thermally Activated Delayed Fluorescence. *Nat. Commun.* **2016**, *7*, 13680.
11. Bergmann, L.; Hedley, G. J.; Baumann, T.; Bräse, S.; Samuel, I. D., Direct Observation of Intersystem Crossing in a Thermally Activated Delayed Fluorescence Copper Complex in the Solid State. *Sci. Adv.* **2016**, *2*, e1500889.
12. Kirchhoff, J. R.; Gamache Jr, R. E.; Blaskie, M. W.; Del Paggio, A. A.; Lengel, R. K.; McMillin, D. R., Temperature Dependence of Luminescence from Cu (Nn) 2+ Systems in Fluid Solution. Evidence for the Participation of Two Excited States. *Inorg. Chem.* **1983**, *22*, 2380-2384.
13. Parker, C.; Hatchard, C., Triplet-Singlet Emission in Fluid Solutions. Phosphorescence of Eosin. *T. Faraday Soc.* **1961**, *57*, 1894-1904.
14. Dias, F. B.; Santos, J.; Graves, D. R.; Data, P.; Nobuyasu, R. S.; Fox, M. A.; Batsanov, A. S.; Palmeira, T.; Berberan-Santos, M. N.; Bryce, M. R., The Role of Local Triplet Excited States and D-A Relative Orientation in Thermally Activated Delayed Fluorescence: Photophysics and Devices. *Adv. Sci.* **2016**, *3*, 1600080.
15. Dias, F. B.; Penfold, T. J.; Monkman, A. P., Photophysics of Thermally Activated Delayed Fluorescence Molecules. *Methods Appl. Fluores.* **2017**, *5*, 012001.
16. Gan, L.; Gao, K.; Cai, X.; Chen, D.; Su, S.-J., Achieving Efficient Triplet Exciton Utilization with LargeΔ Est and Non-Obvious Delayed Fluorescence by Adjusting Excited State Energy Levels. *J. Phys. Chem. Lett.* **2018**.

17. Kobayashi, T.; Niwa, A.; Takaki, K.; Haseyama, S.; Nagase, T.; Goushi, K.; Adachi, C.; Naito, H., Contributions of a Higher Triplet Excited State to the Emission Properties of a Thermally Activated Delayed-Fluorescence Emitter. *Phys. Rev. Appl.* **2017**, *7*, 034002.
18. Kobayashi, T.; Niwa, A.; Haseyama, S.; Takaki, K.; Nagase, T.; Goushi, K.; Adachi, C.; Naito, H., Emission Properties of Thermally Activated Delayed Fluorescence Emitters: Analysis Based on a Four-Level Model Considering a Higher Triplet Excited State. *J. Photon. Energy* **2018**, *8*, 032104.
19. Penfold, T.; Dias, F.; Monkman, A., The Theory of Thermally Activated Delayed Fluorescence for Organic Light Emitting Diodes. *Chem. Commun.* **2018**, *54*, 3926-3935.
20. dos Santos, P. L.; Etherington, M. K.; Monkman, A. P., Chemical and Conformational Control of the Energy Gaps Involved in the Thermally Activated Delayed Fluorescence Mechanism. *J. Mat. Chem. C* **2018**, *6*, 4842-4853.
21. Ogiwara, T.; Wakikawa, Y.; Ikoma, T., Mechanism of Intersystem Crossing of Thermally Activated Delayed Fluorescence Molecules. *J. Phys. Chem. A* **2015**, *119*, 3415-3418.
22. Gibson, J.; Monkman, A. P.; Penfold, T. J., The Importance of Vibronic Coupling for Efficient Reverse Intersystem Crossing in Thermally Activated Delayed Fluorescence Molecules. *ChemPhysChem* **2016**, *17*, 2956-2961.
23. Marian, C. M., Mechanism of the Triplet-to-Singlet Upconversion in the Assistant Dopant Acrxtn. *J. Phys. Chem. C* **2016**, *120*, 3715-3721.
24. Ward, J. S.; Nobuyasu, R. S.; Batsanov, A. S.; Data, P.; Monkman, A. P.; Dias, F. B.; Bryce, M. R., The Interplay of Thermally Activated Delayed Fluorescence (Tadf) and Room Temperature Organic Phosphorescence in Sterically-Constrained Donor–Acceptor Charge-Transfer Molecules. *Chem. Commun.* **2016**, *52*, 2612-2615.
25. Gibson, J.; Penfold, T., Nonadiabatic Coupling Reduces the Activation Energy in Thermally Activated Delayed Fluorescence. *Phys. Chem. Chem. Phys.* **2017**, *19*, 8428-8434.
26. dos Santos, P. L.; Ward, J. S.; Bryce, M. R.; Monkman, A. P., Using Guest–Host Interactions to Optimize the Efficiency of Tadf Oleds. *J. Phys. Chem. Lett.* **2016**, *7*, 3341-3346.
27. Lee, I.; Lee, J. Y., Molecular Design of Deep Blue Fluorescent Emitters with 20% External Quantum Efficiency and Narrow Emission Spectrum. *Org. Electron.* **2016**, *29*, 160-164.

TOC GRAPHIC

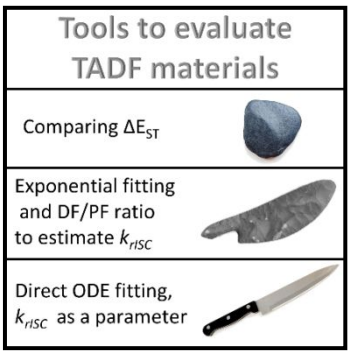
Tools to evaluate TADF materials
Comparing ΔE_{ST}
Exponential fitting and DF/PF ratio to estimate k_{rISC}
Direct ODE fitting, k_{rISC} as a parameter